

# NUMERICAL AND EXPERIMENTAL ANALYSIS OF A DEMAND-SIDE HEAT EXCHANGER FOR DOMESTIC HOT WATER HEATING

Kristen Jaczko<sup>1</sup> Stephen J. Harrison<sup>2</sup>

<sup>1,2</sup>Solar Calorimetry Laboratory, Department of Mechanical and Materials Engineering  
Queen's University, Kingston Ontario, Canada  
k.jaczko@queensu.ca harrison@me.queensu.ca

## ABSTRACT

Natural convection heat exchangers (NCHE) are often used in solar domestic hot water (SDHW) systems as an interface between collector fluid and domestic hot water. This configuration has been thoroughly studied, however NCHEs may be used on the demand-side of storage tanks as a protective measure against harmful legionella bacteria that can multiply in warm water storage systems. In order to predict the performance of demand-side (load-side) NCHEs, the reverse-thermosiphoning process must be characterized. Several tests were carried out on a heat exchanger under a variety of demand-side natural convection conditions. The data set recorded was used to develop empirical characteristic equations governing the relationship between the operating conditions and the performance indices. These equations were implemented in a system-scale TRNSYS model to simulate its performance under representative hot water demand operating conditions.

## INTRODUCTION

Domestic hot water is often stored in large tanks kept at high temperatures (usually above 50°C) in order to mitigate the risk of bacteria growth. Increasingly, there is concern that under certain stratified storage conditions, regions of the storage tank may be at lower temperatures (e.g., 20 to 40°C) which can promote the growth of legionella bacteria [1]. Delivering water in this temperature range could increase the risk of exposure to the bacteria.

One approach thought to minimize the risk is to avoid storing hot potable water and instead heat cold mains water to the desired temperature in a single pass as it is used. This “instantaneous” heating requires significant heating capacity on demand and is difficult to achieve in conventional hot water systems that typically rely on a thermal storage to buffer differences in energy supply and demand frequency (e.g., solar domestic hot water systems).

An alternative configuration, that can still use thermal storage and minimize the risk of delivering insufficiently hot water, uses a demand-side heat exchanger to act as an interface between the storage tank and the domestic hot water load. Heat would be stored in a liquid reservoir and would be delivered through the heat exchanger to the potable water in a single pass as it is consumed. Through this configuration, high levels of thermal stratification in the storage may be used to deliver high temperatures to the load throughout the day.

Heat exchangers are frequently used in solar domestic hot water systems on the collector side of the storage tank. In temperate climates, these systems are used to provide an interface between an anti-freeze solution and the domestic hot water [2]. Several different heat exchangers have been studied for this application and can be classified into two groups: integrated (or internal) heat exchangers and external heat exchangers [2,3].

External heat exchangers have the advantage of being compatible with a large variety of storage tanks and flow through one side of the heat exchanger can be driven by natural convection rather than through the use of a pump [2]. In a study by Harrison and Cruickshank [3] external heat exchangers produced highly stratified thermal storages as well as higher tank temperatures and exergy levels. Charging a tank using an internal heat exchanger, conversely, resulted in the mixing of the tank and consequently lowered tank temperatures and exergy.

Natural convection heat exchangers (NCHE's) have been extensively studied for collector-side applications. Several authors have developed models to predict their performance. Fraser et al. [4] proposed a model based on pressure drop and effectiveness data, which was obtained experimentally. Their procedure required a large number of tests to be run at steady-state for a range of thermosiphon flow rates. Later a modification to this procedure was made in a study by using quasi-steady-state tests. This allowed NCHE's to

be characterized quickly, however it was still necessary to perform a test for each forced-side flow rate [4]. Qin et al. [2] proposed a general model for natural convection heat exchangers that allowed them to be characterized for a full range of flow rates with fewer test runs. Cruickshank [6] further refined and demonstrated the test method and used the results to model the performance of single and multi-tank solar storage systems.

In the present study, the procedure of Qin et al. [2] was applied to a commercially available compact plate heat exchanger. The heat exchanger was used on the load-side of the storage tank in order to facilitate reverse-thermosyphoning. The performance of the heat exchanger was recorded under a variety of forced-side flow rates and initial storage tank temperatures. These results were analyzed to characterize the performance over a range of operating conditions and to produce characteristic equations.

These relationships were then applied in a TRNSYS simulation to test the heat exchanger's performance under standard domestic hot water load conditions.

## BACKGROUND THEORY

The performance of heat exchangers under forced flow conditions has been extensively studied, however their use in natural convection applications on the demand-side of the storage tank has yet to be widely investigated. Typically, the performance of a forced flow heat exchanger is characterized by the effectiveness ( $\epsilon$ ), the capacity ratio ( $C_r$ ) and the number of heat transfer units ( $NTU$ ). The relationship between these variables in a counter flow arrangement is generally expressed as,

$$\epsilon = \frac{1 - \exp[-NTU(1 - C_r)]}{1 - C_r \cdot \exp[-NTU(1 - C_r)]} \quad (1)$$

In a NCHE configuration, temperature/density-induced buoyancy forces drive natural convection on the thermosyphon side of the heat exchanger. The rate of flow in the convection loop is dependent on: the thermal storage temperature; the pressure-drop associated with the heat exchanger and thermosyphon loop; the fluid temperatures inside the exchanger; and, the forced-side fluid capacitance rate [2].

The natural convection or buoyancy-driven flow through the heat exchanger depends on the temperature distribution in the storage tank and consequently, its state of charge. To accommodate the fact that the minimum capacitance rate may change sides during the

charge sequence, a set of modified performance indices were used to characterize natural convection heat exchangers. Specifically, a modified effectiveness ( $\epsilon_{mod}$ ), modified capacity ratio ( $C_{r\ mod}$ ) and modified number of heat transfer units ( $NTU_{mod}$ ) were defined based on the forced-flow capacitance rate rather than the traditional minimum capacitance rate.i.e.,

$$\epsilon_{mod} = \frac{Q_{actual}}{Q_f} = \frac{(\dot{m}_t \cdot C_{pt})(T_{to} - T_{ti})}{(\dot{m}_f \cdot C_{pf})(T_{fi} - T_{ti})} \quad (2)$$

$$NTU_{mod} = \frac{UA}{\dot{m}_f \cdot C_{pf}} \quad (3)$$

$$C_{r\ mod} = \frac{\dot{m}_t \cdot C_{pt}}{\dot{m}_f \cdot C_{pf}} \quad (4)$$

where:  $m_t$  and  $m_f$  are the thermosyphon flow rate and forced flow rate respectively.  $C_{pt}$  and  $C_{pf}$  are the heat capacities of the fluid on the thermosyphon and the forced-side of the heat exchanger respectively. The temperatures at the outlets and inlets of the heat exchanger are represented by  $T_{to}$ ,  $T_{ti}$ ,  $T_{fo}$  and  $T_{fi}$  where subscript  $t$  denotes the thermosyphon loop outlet and inlet temperatures and subscript  $f$  denotes the forced-side outlet and inlet temperatures.  $UA$  is the product of the overall heat transfer coefficient of the heat exchanger and heat transfer area [5].

The thermosyphon flow in a natural convection heat exchanger is dependent on the pressure drop through the thermosyphon loop and heat exchanger, and the net thermosyphon pressure head. The net pressure head in the thermosyphon loop depends on the temperature distribution in the storage tank and thermosyphon loop. The pressure drop in the thermosyphon loop is the sum of the friction losses due to pipe fittings and connections [2].

The natural convection flow rate through the heat exchanger is estimated by assuming that the pressure drop associated with the friction losses (Eq. 5) is in equilibrium with the temperature dependent pressure head (Eq. 6). The net hydrostatic pressure can be found using the following equations.

$$\Delta P = \rho_{to} \cdot g \cdot H_{tank} - H_{HX} + \rho_{\bar{T}_{hx}} \cdot g \cdot H_{HX} - \rho_{\bar{T}_{tank}} \cdot g \cdot H_{tank} \quad (5)$$

$$\Delta P = \rho_{to} \cdot g \left( H_{tank} - \frac{H_{HX}}{2} \right) + \rho_{fi} \cdot g \cdot \frac{H_{HX}}{2} - \rho_{\bar{T}_{tank}} \cdot g \cdot H_{tank} \quad (6)$$

The terms  $\rho_{to}$  and  $\rho_{fi}$  represent the density of the water at the outlet and inlet of the heat exchanger on the storage-side,  $\rho_{T_{tank}}$  and  $\rho_{T_{HX}}$  are the average density of the water in the tank and in the heat exchanger. The dimensions  $H_{tank}$  and  $H_{HX}$  are shown in Fig. 1.

These relationships have been studied and an empirical model has been proposed for the performance of a NCHE, i.e.,

$$\dot{m}_t = a \cdot (\Delta P)^b \quad (7)$$

$$\varepsilon_{mod} = c \cdot (C_{r_{mod}})^2 + d \cdot (C_{r_{mod}}) \quad (8)$$

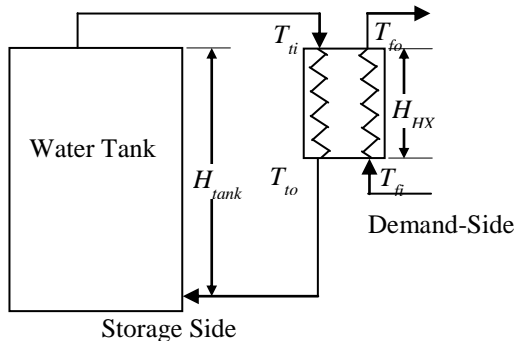


Fig. 1. Demand-side counter-flow heat exchanger.

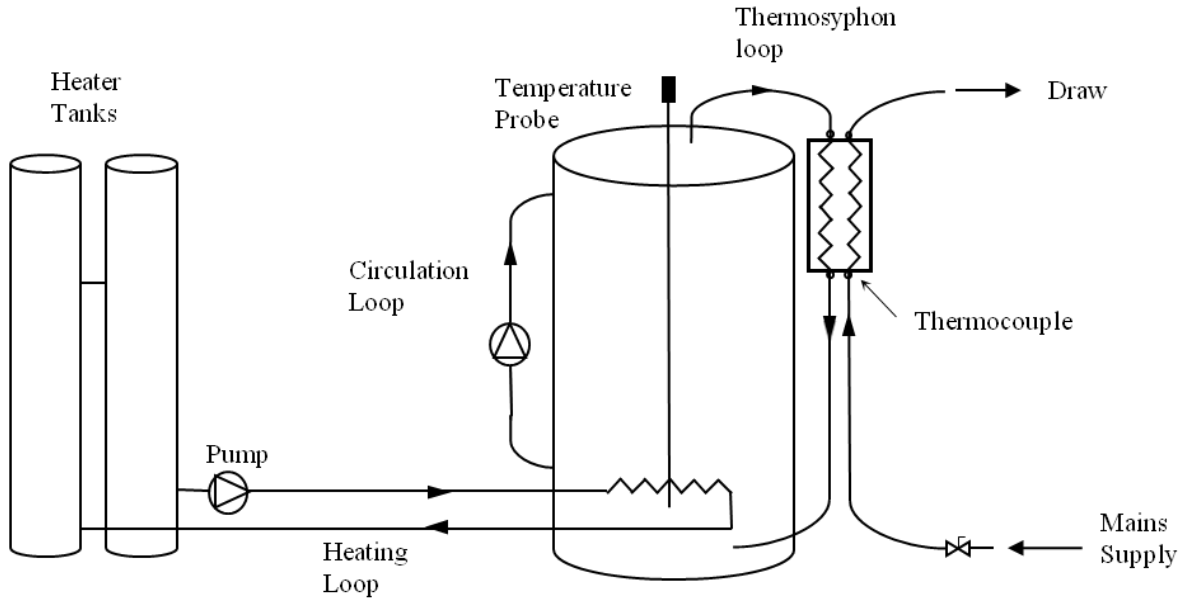


Fig. 2. Schematic of the test apparatus used to evaluate the performance of the heat exchanger.

where the thermosyphon flow rate ( $m_t$ ) has units of  $kg/min$  and  $a$ ,  $b$ ,  $c$ , and  $d$  are constants that can be derived from experimental data.

## METHODOLOGY

The test apparatus used for this study consisted of three parts: a heating loop, a circulation loop and a thermosyphon loop. The heating loop was composed of an internal spiral heat exchanger, inside of a 270 L insulated storage tank, connected to two auxiliary heater tanks and a pump. While the storage tank was charged, a circulation pump mixed the tank to maintain a uniform temperature profile. Once the tank had reached the desired test temperature, the heaters and pumps were turned off and the heating loop was isolated.

At the start of a test sequence, cold water from the local mains supply was run through the forced side of the heat exchanger, in a counter flow arrangement, to replicate the load-side draw. The forced flow rate was recorded with a flow meter. The flow of cold water through the load-side of the heat exchanger cooled the water in the thermosyphon loop, increasing its density and inducing a buoyancy-driven flow in the thermosyphon loop. Temperatures of the inlets and outlets of the heat exchanger, as well as the temperature profile of the storage tank, were recorded using thermocouples. The heat exchanger and all connecting pipes were well insulated to prevent external heat loss. In previous studies, where the

**Table 1. Operation conditions used to evaluate the heat exchanger.**

Test Number	Start Temperature of Tank (°C)	Flow Rate of Mains Water (L/min)	Mains Water Temperature (°C)
1	56	5.47	6.9
2	55	2.1	8.9
3	60	1.95	10.2
4	50	1.25	11.6
5	62	1.05	12.8

NCHE charged the storage tank, the heat exchanger was placed near the bottom of tank. In this study the heat exchanger was located at the top of the thermosyphon loop to facilitate reverse thermosyphoning (Fig. 2).

A temperature probe was used to monitor the temperature profile in the tank at 15 cm intervals. All temperatures and flow rates were recorded at 1.5 minute intervals by a computer based data-acquisition system. The flow rate on the forced-side of the heat exchanger was set at a constant rate during each test. The flow rate of the thermosyphon loop was calculated

by performing an energy balance on the test heat exchanger. The test procedure was repeated for a range of initial storage tank temperatures and load-side flow rates. The experimental set up shown in Fig. 2 was subjected to the operating conditions listed in Table 1.

## RESULTS

A series of tests were performed on a compact plate heat exchanger installed on the load-side of a storage tank to characterize the relationship between the operating conditions and the modified performance parameters of the heat exchanger. The modified

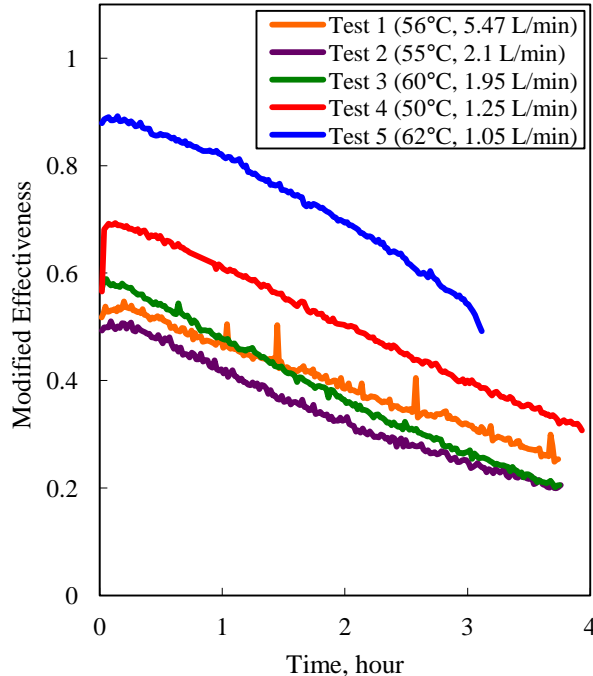


**Fig. 3. Modified effectiveness of the heat exchanger during various tests. Note the initial storage temperature and the mains water flow rate are listed in brackets.**

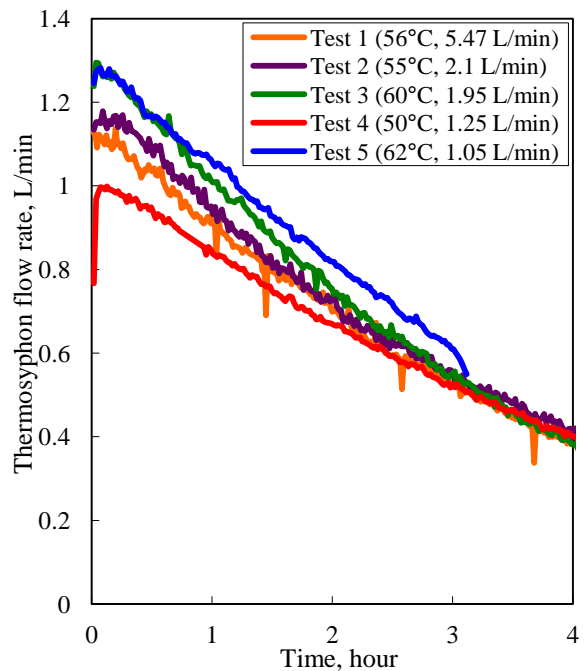


**Fig. 4. Natural convection flow during each test period. Note the initial storage temperature and the mains water flow rate are listed in brackets**

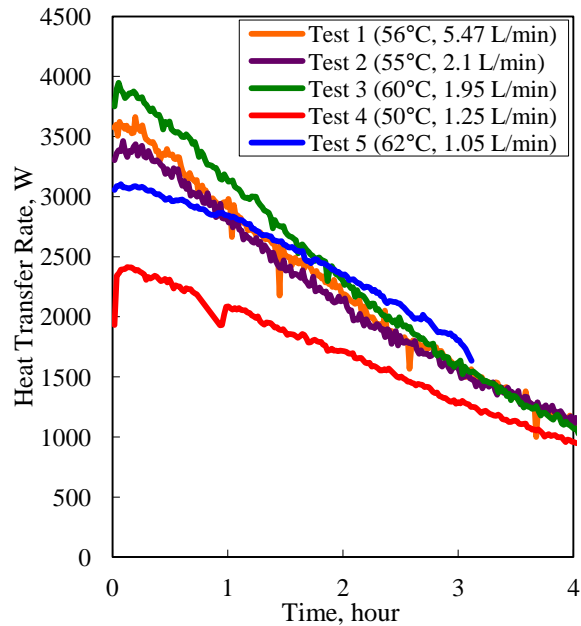


**Fig. 5. Heat transfer rates as measured over the duration of the tests. Note the initial storage temperature and the mains water flow rate are listed in brackets.**

effectiveness, thermosyphon flow rate, and heat transfer rate were determined for each test period. Figure 3 shows the modified effectiveness calculated over the duration of each test. It was evident from the results that, for the configuration tested, the flow rate on the forced side must be low to achieve higher effectiveness values. This was observed in tests 4 and 5 when the flow rate on the demand-side was below 1.5 L/min. Test 5 was performed with the highest initial tank temperature and therefore reached the highest overall modified effectiveness of any of the tests performed.

Figure 4 shows the reduction in the thermosyphon flow rate as the test progressed due to the reduction in tank temperature and thus a reduction in the natural convection driving forces. The initial natural convection flow rate in the tank depended mainly on the starting temperature of the charged storage tank and the temperature of the mains water. This created the pressure gradient that drove the natural convection current. There was no control of the mains water temperature during this study, however it remained relatively constant at the values recorded in Table 1 during each test. Tests 3 and 5 had the highest storage starting temperatures and therefore reached the highest thermosyphon flow rates. In general, it can be seen from Fig. 4 that at higher initial tank temperature resulted in a higher thermosyphon flow rate. Operating

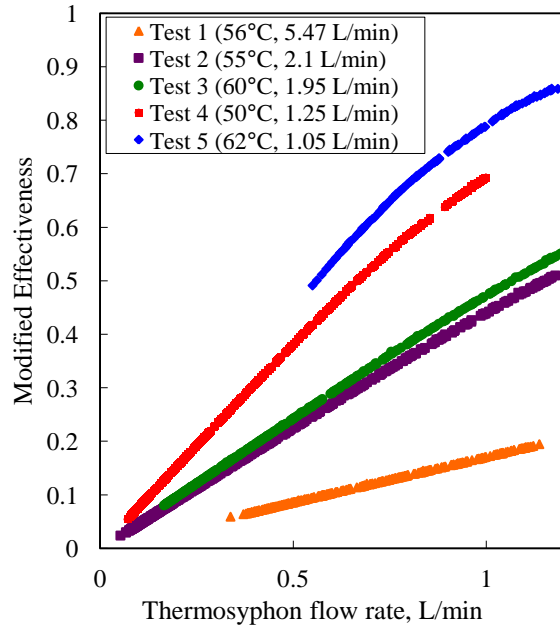


**Fig. 6. The modified effectiveness versus the natural convection flow rate. Note the initial storage temperature and the mains water flow rate are listed in brackets.**

at a significantly lower forced flow rate, the natural convection flow rate during test 2 was slightly higher than the flow rate of test 1. This again demonstrated the impact of the forced flow rate when the initial storage tank temperatures were very similar.

By comparing Figs. 4 and 5 it can also be seen that the heat transfer rate was dependent on the thermosyphon flow rate. During test 5 this was not the case as the limiting factor was the smaller difference in temperatures entering the heat exchanger due to a higher mains water temperature.

## ANALYSIS

The modified effectiveness is plotted against the natural convection flow rate in Fig. 6 to show the relationship between the overall performance of the heat exchanger and the flow rate in the thermosyphon loop. Tests 2 and 3 had similar initial tank temperatures and demand-side flow rates and consequently fell on a very similar curve (Fig. 6). All other tests were run under a wider range of operating conditions and thus fell on separate curves. This demonstrates the dependence of the effectiveness on the forced flow rate as well as the thermosyphon flow rate in the tank. Since the high draw flowrate (i.e., Test 1) experiments had low modified effectiveness values, it was inferred that the natural convection flow rate was not adequate

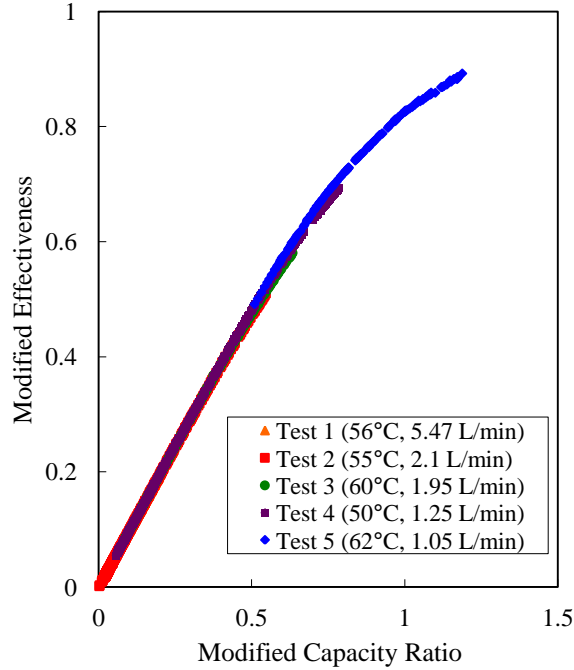


**Fig. 7. Modified effectiveness versus modified capacitance ratio. Note the initial storage temperature and the mains water flow rate are listed in brackets**

to accommodate the high heat transfer rates. This limited the heat exchangers's performance. This would indicate that, at a high forced flow rate, a lower pressure drop would be required in the thermosyphon loop to accommodate a larger tank-side flow rate.

Tank heating natural convection heat exchangers have been characterized in the past by plotting the modified effectiveness against the modified capacitance ratio (Eq. 8). [2] Figure 7 illustrates that this relationship is still valid if the NCHE is used on the load-side of the storage tank. In order to achieve high effectiveness values, the system must be able to achieve comparable flow rates on both the forced and natural convection sides of the heat exchangers. The modified effectiveness curve was found to be a second-order function of the capacitance rate on the demand-side of the heat exchanger and the thermosyphon capacitance rate in the storage loop, as seen below:

$$\varepsilon_{\text{mod}} = -0.229(C_{r_{\text{mod}}})^2 + 1.0577(C_{r_{\text{mod}}}) \quad (9)$$

The form of Eq. 9 was consistent with previous studies using similar flat plate heat exchangers on the supply-side of the tank [5].

Based on these results, a generalized performance model was produced. As previously shown in Eq. 4,

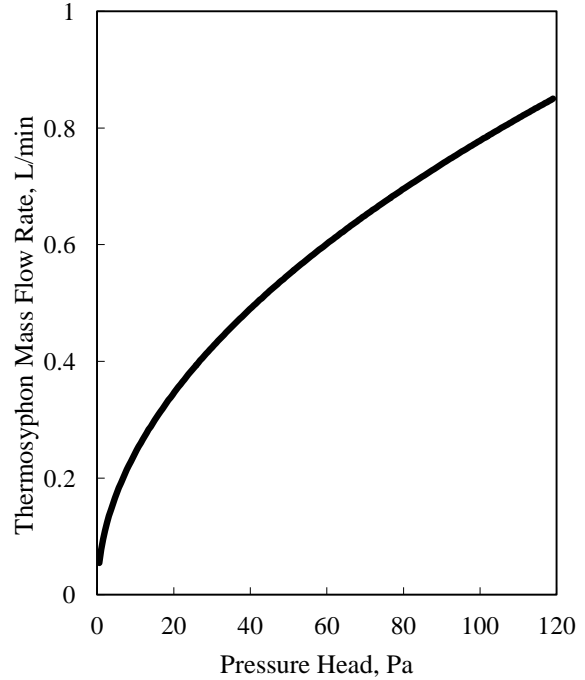


**Fig. 8. Thermosyphon flow rate as a function of pressure head due to the temperature distribution in the storage tank and thermosyphon loop.**

the capacity ratio is a function of the operational conditions of the two fluid streams (i.e., the temperatures and flow rates of these fluids). The flow rate on the load-side of the heat exchanger was simulated using a representative load patterns for domestic hot water use. Therefore in order to obtain the modified capacity ratio it was necessary to calculate the thermosyphon flow rate. As previously stated, this flow rate is dependent on the net pressure head in the thermosyphon loop. NCHE's therefore are also characterized by the relationship between the thermosyphon flow rate and the pressure head associated with the tank and thermosyphon density distribution, as calculated according to Eq. 6. The density of the water in the thermosyphon loop can be calculated using the temperature distribution in the loop. This relationship is expressed as a power function.

$$\dot{m}_s = -0.0762(\Delta P)^{0.5047} \quad (10)$$

With this relationship defined, it was possible to predict the thermosyphon flow rate based on the storage state of charge, the temperature distribution and the forced side flow rate and temperature. It should be noted that the constants of the characteristic equations (Eq.'s 9 and 10), obtained from Fig.'s 7 and 8, were only valid for the set up of the test apparatus used in this study

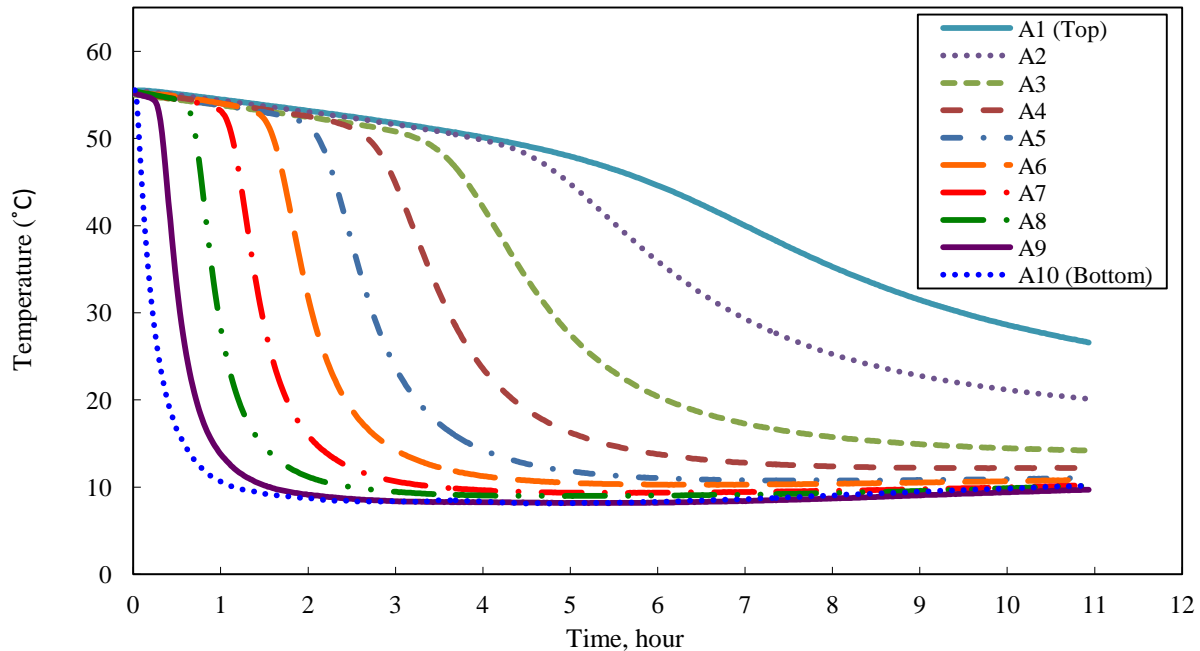


**Fig. 9. Typical storage tank temperature profile during a mains water draw through the demand-side of the NCHE.**

and different results may be obtained for other geometries and heat exchangers. A typical temperature profile of the storage tank was plotted in order to illustrate the effect of the reverse thermosyphoning on the stratification of the tank. Figure 9 shows that the tank was uniform in temperature at the beginning of the test. As the demand-side flow commenced, the temperature at the bottom of the tank dropped rapidly, followed by each higher layer.

### SIMULATION

In order to properly size a heat exchanger for use in a domestic hot water system, it is necessary to simulate the system under typical load conditions. This analysis was completed for a desired draw temperature of 55°C. The storage tank in this simulation was electrically heated. The TRNSYS two components, created by Cruickshank [6] to model NCHE on the supply-side of the storage tank, were modified to facilitate the reverse thermosyphoning process. These components use Eq.'s 7 and 8 to simulate the performance of the NCHE based on the operating conditions. The constants,  $a$ ,  $b$ ,  $c$  and  $d$ , from Eq's 9 and 10 were input into the components as parameters. The first component used the temperature distribution in the thermosyphon loop to calculate the density and thus find the pressure drop according to Eq. 6. This was then used in Eq. 10 to find the thermosyphon flow rate that would result from this driving pressure. The second component used the

thermosyphon flow rate, forced flow rate and assumed average heat capacities for both fluids. From Eq. 9 the effectiveness was found and thus the outlet temperatures of the heat exchanger were also calculated.

A typical draw schedule for a daylong simulation, shown in Fig. 10, demonstrates that the desired hot water temperature was only reached for the lower flow draws of DHW. Therefore the heat exchanger used in this study would not be suitable for this particular application. The results of this simplified model showed that simulation of a full domestic hot water supply system, with a natural convection heat exchanger used on the demand-side, can be performed using the characteristic equations obtained from experimentation. The demand for domestic hot water (DHW) is shown in blue (long dashed line), the flow rate in the tank is represented by the yellow line (short dashed line) and the temperature delivered to meet the demand is shown in red (solid line).

### CONCLUSIONS

A compact heat exchanger was used on the load-side of a storage tank under natural convection conditions. Cold mains water was run through one side of the heat exchanger at different flow rates and storage tank initial temperatures. The heat exchanger's performance

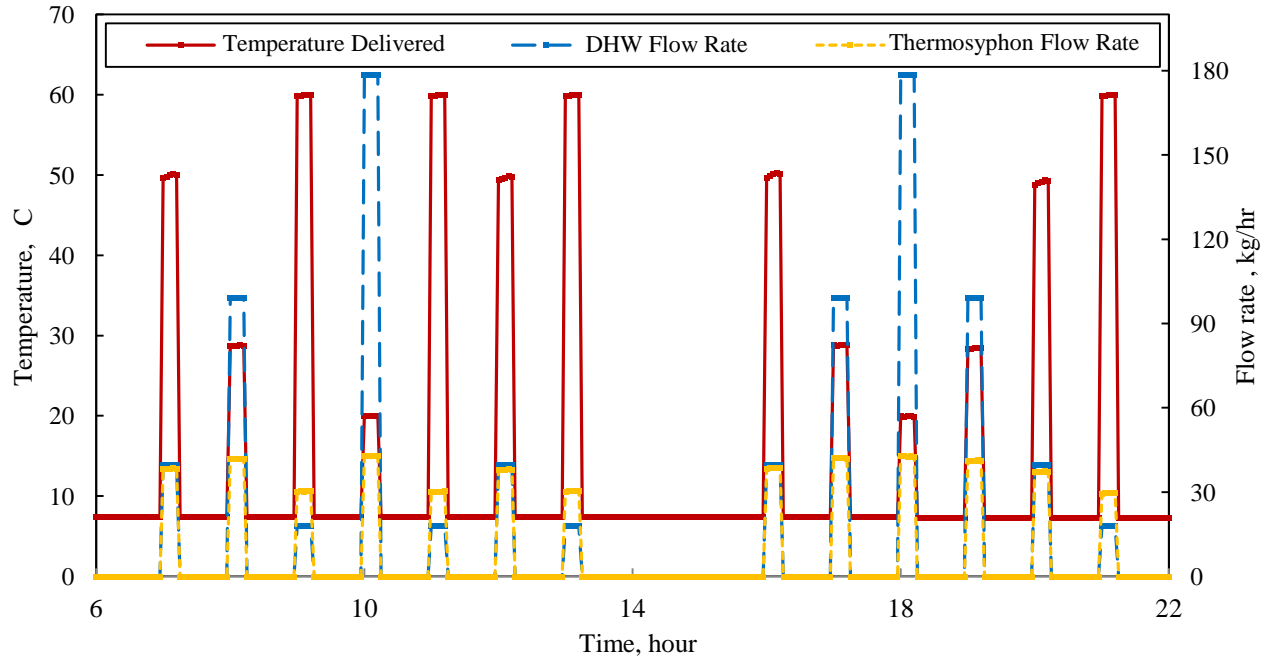


**Fig. 10. TRNSYS simulation of the heat exchanger and storage tank under typical load conditions.**

was recorded under this range of operating conditions and analyzed to produce a model capable of predicting the performance of a particular heat exchanger and storage tank configuration.

As expected, based on an analysis of previous studies on supply side NCHEs, the performance of the heat exchanger could be predicted using the operating conditions. The thermosyphon flow rate was shown to be a function of the net pressure head in the thermosyphon loop. The pressure head was found from the temperature distribution in the storage tank and thermosyphon loop. The natural convection flow rate and forced flow rate were then used to find the modified capacity ratio and effectiveness based on the experimentally derived coefficients of the characteristic equations for heat exchanger configuration tested.

The results of this testing also indicated that the configuration tested was not optimum for high forced-flow cases and its performance was limited by the mismatch between forced and natural convection flow rates. Higher storage tank temperatures and lower pressure drop through the thermosyphon loop would reduce these effects.

The results of this study have demonstrated the possibility of using a load-side heat exchanger in a single-pass configuration. One of the most interesting observations of this work is that the load side heat exchanger case studied is very similar the charge-side

cases previously studied except that the temperature gradients are reversed.

#### ACKNOWLEDGEMENTS

This research was supported by the NSERC Smart Net-Zero Energy Buildings Strategic Research Network (SNEBRN). The authors also wish to acknowledge the assistance of Mr. Gary Johnson in setting up the apparatus and test procedure.

#### NOMENCLATURE

$\varepsilon$	Heat exchanger effectiveness	
$C_r$	Capacity ratio	
$NTU$	Number of heat transfer units	
$\varepsilon_{mod}$	Modified effectiveness	
$C_{r,mod}$	Modified capacity ratio	
$NTU_{mod}$	Modified number of heat transfer units	
$t$	Thermosyphon flow rate	kg/s
$f$	Forced flow rate	kg/s
$C_{pt}$	Heat capacity of the storage fluid	J/kg °C
$C_{pf}$	Heat capacity of the forced fluid	J/kg °C
$T_{to}$	Temperature of thermosyphon fluid leaving the heat exchanger	°C

$T_{ti}$	Temperature of thermosyphon fluid entering the heat exchanger	$^{\circ}\text{C}$
$T_{fo}$	Temperature of forced flow fluid leaving the heat exchanger	$^{\circ}\text{C}$
$T_{fi}$	Temperature of forced flow fluid entering the heat exchanger	$^{\circ}\text{C}$
$UA$	Overall heat transfer coefficient of the heat exchanger	$\text{W}/^{\circ}\text{C}$
$\Delta P$	Net hydrostatic pressure	$\text{Pa}$
$g$	Acceleration due to gravity	$\text{m}/\text{s}^2$
$\rho_{to}$	Density of fluid at the outlet on the storage side of the heat exchanger	$\text{kg}/\text{m}^3$
$\rho_{ti}$	Density of fluid at the inlet on the storage side of the heat exchanger	$\text{kg}/\text{m}^3$
$\rho_{Tank}$	Average density of fluid in the storage tank	$\text{kg}/\text{m}^3$
$\rho_{THX}$	Average density of fluid inside heat exchanger on the storage side	$\text{kg}/\text{m}^3$
$H_{tank}$	Height of the tank	$\text{m}$
$H_{HX}$	Height of the heat exchanger	$\text{m}$

## REFERENCES

[1] J.P. Angermann, M. Izard, C.M. Joppolo, S. La Mura, and L. Alberto, *Legionellosis Prevention in Building Water and HVAC Systems*, 1st ed., S. La Mura, L. Alberto C.M. Joppolo, Ed.: REHVA, 2013.

[2] Q. Lin, S. Harrison, and M. Lagerquist, "Analysis and Modeling of Compact Heat Exchangers," in *EuroSun Conference*, Copenhagen, 2000.

[3] S. Harrison and C. Cruickshank, "Effects of Heat Exchanger Configurations on Solar Domestic Hot Water System Performance," in *ISES Solar World Congress*, Kassel, Germany, 2011.

[4] K.F. Fraser, K.G.T. Hollands, and A.P. Brunger, "An Empirical Model for Natural Convection Heat Exchangers in Solar Heating Systems," *Solar Energy*, vol. 55, no. 2, pp. 75-84, 1995.

[5] S. Harrison, J.M. Purdy, and P.H. Oosthuizen, "Thermal Evaluation of Compact Heat Exchangers in a Natural Convection Application," in *International Heat Transfer Conference*, Kyongju, Korea, 1998, pp. 305-310.

[6] C. Cruickshank, "Evaluation of a Stratified Multi-tank Thermal Storage for Solar Heating Application," Queen's University, Kingston, ON, Canada, Ph.D. dissertation 2009.

[7] S. A. Klein, *TRNSYS: A Transient Simulation Program*, 16th ed. Madison, Wisconsin, Wisconsin, USA: University of Wisconsin Solar Energy Laboratory, 2006.

[8] National Instruments LabVIEW, *LabVIEW*, 80th ed. Austin, TX, Texas, USA, 2005.